Optimal CT Contrast Enhancement Protocol for the Fontan Pathway: An Analysis Based on a 15-year Single-center Experience

Hyun Woo Goo (ghw68@hanmail.net)
Asan Medical Center, University of Ulsan College of Medicine

Research Article

Keywords: Cardiothoracic CT, Contrast enhancement protocol, Fontan pathway, Optimal contrast enhancement, Scan delay

Posted Date: June 17th, 2021

DOI: https://doi.org/10.21203/rs.3.rs-621039/v1

Abstract

This retrospective study was performed to systemically compare several candidates for optimal contrast enhancement protocols of cardiothoracic CT dedicated for evaluating the Fontan pathway. Of 115 CT examinations from 89 patients, simultaneous injection of contrast agent via the arm and leg veins with 50% diluted contrast agent (group 1, *n* = 38), 60-second scan delay after leg vein injection (group 2, *n* = 41) or 3-minute scan delay (group 3, *n* = 36) was used to obtain optimal contrast enhancement. The degree and heterogeneity of cardiovascular enhancement, image noise, signal-to-noise ratio (SNR), and contrast-to-noise ratio (CNR) were quantitatively evaluated. Histogram-assisted semi-quantitative evaluation was performed for heterogeneous enhancement, and a cut-off value indicating heterogeneous enhancement was determined by comparing the standard deviations between the cases showing homogeneous and heterogeneous enhancement. Contrast enhancement of the Fontan pathway, the standard deviation measured in the Fontan pathway, SNR, and CNR were more frequently lower in group 3 compared to groups 1 and 2 ($p < 0.001$). Homogeneous enhancement of the Fontan pathway based on the histogram-assisted semi-quantitative evaluation was more frequently seen in group 3 compared to groups 1 and 2 ($p < 0.043–0.001$). Receiver operating characteristic curve analysis demonstrated that the standard deviation was an excellent diagnostic test in determining the homogeneity of contrast enhancement (area under the curve = 0.991; 95% confidence interval, 0.988–0.994; $p < 0.001$). Standard deviations > 105.1 HU could be considered to indicate heterogeneous enhancement with 73.2% sensitivity and 100.0% specificity. The protocol using a 3-minute scan delay best achieved homogeneous contrast enhancement in the Fontan pathway on cardiothoracic CT among the tested protocols. However, low contrast enhancement, SNR, and, CNR need to be improved.

Introduction

Cardiothoracic CT is frequently requested for identifying stenosis and thromboembolism in the Fontan pathway [1]. It is also often used as an alternative imaging modality in cases with contraindications to cardiac MRI, including MR-incompatible cardiac pacemakers and defibrillators and claustrophobia, and severe artifacts from metallic implants [2, 3]. However, it is quite challenging to achieve homogeneous contrast enhancement in the Fontan pathway on cardiothoracic CT due to turbulent and preferential non-pulsatile flow as clearly demonstrated in time-resolved MRA [4] and four-dimensional flow MRI [5]. The typical contrast enhancement protocols used to evaluate congenital heart disease almost always result in non-uniform, non-diagnostic contrast enhancement on cardiothoracic CT; therefore, additional delayed scanning is often required in patients with the Fontan pathway. Consequently, several contrast enhancement protocols dedicated to evaluate the Fontan pathway on cardiothoracic CT have been suggested [6–12]. An expert consensus document recommended a venous two-phase or split injection method, in which 30–50% of the contrast agent is given and followed by a 30–60 seconds pause and then by the second injection of contrast agent [13]. Another expert consensus guideline recommended a 60–70-second delayed scanning because the method appears to offer balanced opacification of all thoracic cardiovascular structures and requires a simple injection technique [14]. However, systematic

comparisons between the dedicated contrast enhancement protocols for cardiothoracic CT after the Fontan operation have been seldom conducted to determine the best contrast enhancement protocol. Contrast enhancement protocols dedicated to evaluate the Fontan pathway have also been developed and used in our institution since 2006. Therefore, this retrospective study was performed to systematically compare several candidates for optimal contrast enhancement protocols of cardiothoracic CT dedicated to evaluate the Fontan pathway performed for 15 years in our institution and suggest the best alternative.

Materials And Methods

This retrospective study was approved and the requirement for informed consent was waived by the local Institutional Review Board.

Patient Population

For 15 years since 2006, 97 consecutive patients underwent cardiothoracic CT after the Fontan operation using one of three dedicated contrast enhancement protocols in our institution. Eight patients were excluded from this study because they had the following reasons substantially affecting cardiovascular enhancement of the Fontan pathway: inferior vena cava (IVC) interruption with azygos continuation (n = 5); failed intravenous injection of contrast agent (n = 2); and the use of a central venous catheter placed in the superior vena cava (SVC) for injection (n = 1). Therefore, 89 patients were included in this study; a single CT scan was performed in 63 patients; early- (60-second delay) and late- (3-minute delay) phase scans were performed in 26 patients. According to the contrast enhancement protocols, 115 CT examinations from 89 patients were divided into three groups as follows: group 1, simultaneous injection of the contrast agent via the arm and leg veins with 50% diluted contrast agent in 38 examinations; group 2, a 60-second scan delay after leg vein injection at slow injection rates for 55 seconds and stopping the injection 5 seconds before starting the scan in 41 examinations; and group 3, a 3-minute scan delay irrespective of the intravenous injection sites at slow injection rates for 55 seconds in 36 examinations. The demographics and clinical characteristics of the study population are described in Table 1.

Cardiothoracic CT

For the 15 years, cardiothoracic CT examinations were performed using one of three different CT scanners as follows: a 16-slice CT scanner (SOMATOM Sensation 16; Siemens Healthineers), a first-generation dual-source CT scanner (SOMATOM Definition; Siemens Healthineers), and a second-generation dual-source CT scanner (SOMATOM Definition Flash; Siemens Healthineers); and one of which was assigned as a cardiovascular CT scanner in our institution depending on the time period. The scanning technique was determined based on the clinical requests and patients' conditions [15]. Body size-adapted CT scan protocols [15-17] and an attenuation-based tube current modulation (CARE Dose 4D; Siemens Healthineers) [18, 19] were used to optimize the radiation dose. Electrocardiography (ECG)-controlled tube current modulation (MinDose; Siemens Healthineers) and the biphasic chest pain protocol were used to further reduce the radiation dose of the retrospectively ECG-gated spiral scan [20]. When

available, an iterative reconstruction algorithm was used to reduce the image noise while maintaining the image details [21-24]. The scan range included the whole thorax in all patients. Patients younger than 6 years of age were initially sedated with oral chloral hydrate (50 mg/kg) and subsequently with intravenous midazolam (0.1 mg/kg) or ketamine (1 mg/kg) as required. The CT scan was performed during free breathing in these sedated patients or while the conscious and cooperative patients were holding their breath. The presence of metallic implants, such as cardiac pacemakers and vascular coils, on the CT scout images was recorded.

To maximize the radiation dose efficiency and the iodine contrast-to-noise ratio (CNR), the lowest possible tube voltage was selected (Table 2). The volume CT dose index and dose-length product values based on a 32-cm phantom were recorded. The effective dose estimate was calculated by multiplying the dose-length product and the age, sex, and tube voltage-specific conversion factors for the chest CT [16]. The detailed CT parameters are described in Table 2.

Iodinated contrast agent (Iopamidol; Pamiray-370, Dongkook Pharmaceutical; 2.0 mL/kg) was administered intravenously with a dual-head power injector at an injection rate of 0.5 – 2.5 mL/s. The scan delay time was determined by a bolus tracking technique in 17 of 38 CT examinations of group 1, while a fixed delay of either 60 seconds or 3 minutes was used for the remaining CT examinations.

Quantitative Evaluation of the Image Quality

To quantitatively evaluate the degree and heterogeneity of cardiovascular enhancement, image noise, signal-to-noise ratio (SNR), and CNR, a biggest possible region of interest was placed in the right and left internal jugular veins, right and left SVC, right and left pulmonary arteries, inferior cavopulmonary connection, IVC, ascending aorta, ventricle, atrium, ventricular myocardium, and air. When a vessel was not visualized or contained a vascular catheter, CT densitometry could not be performed and these vessels were treated as having missing values. Mean CT density and standard deviation were measured for each location.

Contrast enhancement < 200 Hounsfield units (HU) was regarded to be suboptimal. The standard deviation of the measured air density was regarded as the image noise because it is less affected by different tube voltages. Image noise ≥ 10 HU was regarded to be suboptimal. SNR was calculated using the following formula: SNR = mean density of the ventricle/image noise. CNR was calculated using the following formula: CNR = (mean density of the ventricle - mean density of the ventricular myocardium)/image noise. SNR < 35 and CNR < 20 were regarded to be suboptimal.

Semi-quantitative Evaluation of Heterogeneous Enhancement

There is no established objective criterion indicating heterogeneous enhancement, and the subjective evaluation of heterogeneous enhancement is considerably influenced by the window settings of the CT images (Fig. 1). Therefore, the evaluation in this study was assisted by the shape of the histogram of the obtained CT densitometry. When a histogram showed a single peak with a narrow base, the contrast

enhancement was regarded to be homogeneous (Fig. 2). In contrast, contrast enhancement was regarded to be heterogeneous when a histogram demonstrated a broad-based peak (Figs. 3, 4). The standard deviations were compared between the cases showing homogeneous and heterogeneous contrast enhancement to determine a cut-off value indicating heterogeneous contrast enhancement.

Statistical Analysis

Continuous variables are presented as mean ± standard deviation or median with range, and categorical variables are expressed as frequencies with percentages. For the comparisons of the continuous variables between the groups, an unpaired *t*-test was used. A chi-square test or Fisher's exact test was used for the comparisons of the categorical variables between the groups, depending on whether the expected cell counts were below five or not. Receiver operating characteristic (ROC) curve analysis was used to assess the diagnostic ability of a binary classifier system (heterogeneous or homogeneous contrast enhancement). A *p*-value less than 0.05 was considered statistically significant. Statistical analyses were performed using statistical software (SPSS version 24.0; IBM Corp., Armonk, NY, USA).

Results

Patient Population

No significant differences were found in the age and sex ratio between the groups ($p > 0.365$–0.728 and $p > 0.081$, respectively) (Table 1). Among the three modifications of the Fontan operation, the extracardiac conduit type was the most common in the range of 84.2–97.6% in all three groups (Table 1). Metallic implants producing severe beam hardening artifacts were frequently present in the range of 16.7–22.2% in the three groups (Table 1).

Cardiothoracic CT

The non-ECG-synchronized spiral scan was most frequently performed in the initial period (2006–2014) of this study, while the ECG-synchronized scans prevailed in the later period (Table 2). Similarly, lower tube voltages including 70 kV and 80 kV were more frequently selected in a later period of this study (Table 2). The dose-length product and effective dose in group 3 were significantly lower than those in group 1 ($p < 0.046$ and $p < 0.012$, respectively), whereas radiation dose metrics showed no significant differences in other comparisons ($p > 0.060$–0.522) (Table 2).

Quantitative Evaluation of the Image Quality

The results of the quantitative evaluation of the image quality are described in Table 3. The mean densities in group 3 were significantly lower than those in groups 1 and 2 in all the cardiovascular structures ($p < 0.001$–0.005), except for the left SVC in which the mean density in group 1 was significantly higher than those in groups 2 and 3 ($p < 0.005$ and $p < 0.043$, respectively) (Table 3). The mean densities of the IVC and inferior cavopulmonary connection in group 2 were significantly higher than those in groups 1 and 3 ($p < 0.001$) (Table 3). In contrast, the mean density of the myocardium

showed no significant differences among the three groups ($p > 0.212–934$) (Table 3). Suboptimal contrast enhancement (< 200 HU) was more frequently seen in the IVC, pulmonary arteries, ascending aorta, ventricle, and atrium in group 3 than in groups 1 and 2 ($p < 0.001–0.048$) (Table 3).

The standard deviations of the CT densitometries in group 3 were significantly lower than those in groups 1 and 2 in the internal jugular veins, vena cavae, inferior cavopulmonary connection, and pulmonary arteries ($p < 0.001–0.016$) (Table 3). In the ventricle, the standard deviation of CT densitometry was significantly lower in group 1 than those in groups 2 and 3 ($p < 0.001$ and 0.017, respectively) (Table 3). In the atrium, the standard deviation of CT densitometry was significantly higher in group 2 than those in groups 1 and 3 ($p < 0.001$) (Table 3). In contrast, the standard deviations of CT densitometries measured in the ascending aorta and myocardium showed no significant differences among the three groups ($p > 0.063–0.473$ and $p > 0.128–0.612$) (Table 3).

Image noise measured in the air in group 1 was significantly lower than those in groups 2 and 3 ($p < 0.017$ and 0.001, respectively), while image noises were comparable between groups 2 and 3 ($p > 0.141$) (Table 3). In all three groups, suboptimal image noise (≥ 10 HU) was rarely observed in the range of 0.0–7.3% without significant differences in frequency ($p > 0.233$) (Table 3). Notably, SNR and CNR in group 3 were significantly lower than those in groups 1 and 2 ($p < 0.001$), while they were comparable between groups 1 and 2 ($p > 0.196$ and $p > 0.114$, respectively) (Table 3). The proportions of suboptimal SNR (< 35) and CNR (< 20) were also significantly higher in group 3 than in groups 1 and 2 ($p < 0.001$), while they were comparable between groups 1 and 2 ($p > 0.676$) (Table 3).

Semi-quantitative Evaluation of Heterogeneous Enhancement

In the internal jugular veins, the homogeneities of contrast enhancement were significantly higher in group 3 than in group 1 ($p < 0.006$) (Table 3), while groups 2 and 3 demonstrated comparable homogeneities ($p > 0.244$) (Table 3). In the SVCs, the homogeneities of contrast enhancement were significantly different among the three groups ($p < 0.043$): the highest in group 3, followed by group 2 and then group 1 (Table 3). In the IVC, inferior cavopulmonary connection, and pulmonary arteries, the homogeneities of contrast enhancement were significantly higher in group 3 than in groups 1 and 2 ($p < 0.001$) (Table 3), while groups 1 and 2 demonstrated comparable homogeneities ($p > 0.086$) (Table 3). In the ascending aorta, ventricle, and atrium, there were no significant differences in the homogeneities of contrast enhancement among the three groups ($p > 0.055$) and they were 100% in all, except for the atrium in group 2 (87.8%) (Table 3). Notably, group 3 frequently showed 100% homogeneity in all cardiovascular structures, except for the IVC (80.6%) and inferior cavopulmonary connection (91.7%) (Table 3).

In the three groups, contrast enhancement was homogeneous in 863 cardiovascular structures and heterogeneous in 284 cardiovascular structures. The standard deviations in the cases showing heterogeneous enhancement were significantly higher than those in the cases showing homogeneous enhancement (196 ± 110.4 HU vs. 25.4 ± 16.9 HU, $p < 0.001$). ROC curve analysis demonstrated that the standard deviation measured in the cardiovascular structures was an excellent diagnostic test in

determining homogeneity of contrast enhancement (area under the curve = 0.991; 95% confidence interval, 0.988–0.994; p < 0.001) (Fig. 5). With a cut-off value of 105.1 HU, higher standard deviations could be considered to indicate heterogeneous enhancement with 73.2% sensitivity and 100.0% specificity.

Discussion

Based on the quantitative and semi-quantitative results of this study, the 3-minute delayed scanning (group 3) demonstrated the most homogeneous contrast enhancement in the Fontan pathway compared to the other contrast enhancement protocols (groups 1 and 2). In contrast, contrast enhancement, SNR, and CNR were lowest in group 3 compared to groups 1 and 2. These findings are similar to those reported in a previous study evaluating 88 CT examinations in 49 consecutive patients who underwent the Fontan operation [8]. However, the current study demonstrated substantially higher mean CT density values in the aorta, Fontan tract, and pulmonary artery on 3-minute delayed CT examinations than the previous study (237.7 HU vs. 165.6–178.6 HU, 237.9 HU vs. 160.1–166.2 HU, and 220.5–223.2 HU vs. 162.1–165.1 HU, respectively) [8]. The differences in the measured CT densities between the two studies might be attributed mainly to more frequent use of higher tube voltage (i.e., 80 kV for patients < 40 kg and 120 kV for patients ≥ 40 kg) in the previous study [8] than in the current study (i.e., 70 kV in 10.4% [12/115], 80 kV in 60.0% [69/115], 100 kV in 27.8% [32/115], and 120 kV in only 1.7% [2/115]) (Table 2).

In addition, the authors of the previous study [8] considered that the mean CT densities of 160 to 170 HU were in the subjectively acceptable range of contrast enhancement to evaluate the Fontan pathway, whereas the acceptable level (200 HU) of contrast enhancement was slightly higher in the current study. Even though the authors stated that all images using the 3-minute-delay scan achieved acceptable enhancement of all three vascular structures including the aorta, pulmonary artery, and Fontan tract, a substantial proportion of the CT images obtained at the 3-minute delay might show insufficient contrast enhancement based on the mean attenuations in the range of 160.1–166.2 HU and the standard deviations in the range of 25.1–42.3 HU, except for the aorta in cases using a foot vein root [8]. Moreover, the normal myocardium also showed contrast enhancement on delayed CT scans [25]. The mean myocardial attenuation measured on the delayed (1 minute to 3 minutes) CT scans was 142.1–151.8 HU (Table 3). Therefore, the CNR of the 3-minute-delay scans that was not calculated in the previous study [8] was expected to be insufficiently low for evaluating intracardiac morphology accurately. In the current study, 94.4% of the cases obtained using the 3-minute delay (group 3) showed suboptimal CNR (< 20) (Table 3).

Consequently, the CNR of the 3-minute-delay scans needs to be further improved. One way of increasing the CNR is by using a shorter scan delay, but the 60-second delay seemed to lead to inhomogeneous enhancement in the Fontan pathway based on the results of this study. Some researchers suggested a 70-second delay [1, 12] and others suggested an 80–100 second delay [10]. However, it should be carefully considered that heterogeneity of contrast enhancement in the Fontan pathway seems to be increased proportional to the shortening of the scan delay. Therefore, further studies are warranted to

determine how the scan delay may be shortened from 3 minutes without compromising homogeneous enhancement in the Fontan pathway. Another potential method of increasing the CNR of the 3-minute-delay scans is by using virtual monoenergetic image reconstruction at low keV using dual-energy CT scanning [26, 27].

Objective evaluation of homogeneous contrast enhancement in the Fontan pathway is challenging. For example, visual evaluation is considerably affected by the window setting of the CT images as was demonstrated in Figure 1 of the current study. Nevertheless, subjective evaluation of homogeneous enhancement in the Fontan pathway has been frequently used [8, 9]. To avoid visual perception errors, the standard deviation of the measured CT attenuation in the cardiovascular structures by placing a region of interest is infrequently used to represent a quantitative measure of homogeneity in contrast enhancement. Among seven different contrast enhancement protocols, the standard deviations of the aorta, pulmonary artery, and Fontan tract were less than 30 HU in the 1-minute-delay scan with both antecubital routes and the 3-minute-delay scan, irrespective of the intravenous injection sites [8]. Other protocols demonstrated higher standard deviations of the pulmonary artery and Fontan tract (up to 76 HU and 504 HU, respectively) [8]. However, the standard deviation (30 HU) used for the criteria of heterogeneous enhancement in their study [3] was rather arbitrary without any solid evidences. In addition, they used a fixed size (30 mm^2) in the area of the regions of interest, irrespective of the sizes of the vessels, and therefore, they might have selected areas of relative homogeneous enhancement in the vessels for the measurements [8]. In contrast, the region of interest used in this study included the whole area of the vessels to avoid selection bias in the measurements. In addition, the patterns of the histogram of CT densitometry were used to minimize pitfalls of qualitative evaluation of homogeneous contrast enhancement solely depending on human eyes and substantial changes in enhancement pattern by changing window settings of the CT images. According to the ROC curve analysis, the standard deviation of 105.1 HU may be served as a useful cut-off value in determining homogeneity of contrast enhancement.

This study had several limitations. First, it is impossible to completely avoid selection bias in the patient population due to its retrospective nature. Second, the study population was relatively small.

Conclusions

The contrast enhancement protocol using a 3-minute scan delay is the best to achieve homogeneous contrast enhancement in the Fontan pathway on cardiothoracic CT among the tested protocols. However, low contrast enhancement, SNR, and CNR need to be improved.

Declarations

Compliance with ethical standards

Conflict of interest All authors declare that they have no financial or non-financial conflict of interest.

Ethical approval All procedures performed were in accordance with the ethical standards of the institutional research committee and with the 1964 Helsinki declaration and its later amendments or comparable ethical standards.

References

1. Ghadimi Mahani M, Agarwal PP, Rigsby CK, Lu JC, Fazeli Dehkordy S, Wright RA, Dorfman AL, Krishnarmurthy R (2016) CT for assessment of thrombosis and pulmonary embolism in multiple stages of single-ventricle palliation: challenges and suggested protocols. Radiographics 36 (5):1273–1284. https://doi.org/10.1148/rg.2016150233
2. Han BK, Lesser JR (2013) CT imaging in congenital heart disease: an approach to imaging and interpreting complex lesions after surgical intervention for tetralogy of Fallot, transposition of the great arteries, and single ventricle heart disease. J Cardiovasc Comput Tomogr 7 (6): 338–353. https://doi.org/10.1016/j.jcct.2013.10.003
3. Ranganath P, Singh S, Abbara S, Agarwal PP, Rajiah P (2019) Computed tomography in adult congenital heart disease. Radiol Clin North Am 57 (1):85–111. https://doi.org/10.1016/j.rcl.2018.08.013
4. Goo HW, Yang DH, Park IS, Ko JK, Kim YH, Seo DM, Yun TJ, Park JJ (2007) Time-resolved three-dimensional contrast-enhanced magnetic resonance angiography in patients who have undergone a Fontan operation or bidirectional cavopulmonary connection: initial experience. J Magn Reson Imaging 25 (4):727–736. https://doi.org/10.1002/jmri.20870
5. Jarvis K, Schnell S, Barker AJ, Garcia J, Lorenz R, Rose M, Chowdhary V, Carr J, Robinson JD, Rigsby CK, Markl M (2016) Evaluation of blood flow distribution asymmetry and vascular geometry in patients with Fontan circulation using 4-D flow MRI. Pediatr Radiol 46 (11):1507–1519. https://doi.org/10.1007/s00247-016-3654-3
6. Greenberg SB, Bhutta ST (2008) A dual contrast injection technique for multidetector computed tomography angiography of Fontan procedures. Int J Cardiovasc Imaging 24 (3):345–348. https://doi.org/10.1007/s10554-007-9259-z
7. Prabhu SP, Mahmood S, Sena L, Lee EY (2009) MDCT evaluation of pulmonary embolism in children and young adults following a lateral tunnel Fontan procedure: optimizing contrast-enhancement techniques. Pediatr Radiol 39 (9):938–944. https://doi.org/10.1007/s00247-009-1304-8
8. Park EA, Lee W, Chung SY, Yin YH, Chung JW, Park JH (2010) Optimal scan timing and intravenous route for contrast-enhanced computed tomography in patients after Fontan operation. J Comput Assist Tomogr 34 (1) (2010) 75–81. https://doi.org/10.1097/RCT.0b013e3181ae292c
9. Sandler KL, Markham LW, Mah ML, Byrum EP, Williams JR (2014) Optimizing CT angiography in patients with Fontan physiology: single-center experience of dual-site power injection. Clin Radiol 69 (12):e562–e567. https://doi.org/10.1016/j.crad.2014.09.011

10. Loughborough WW, Yeong M, Hamilton M, Manghat N (2017) Computed tomography in congenital heart disease: how generic principles can be applied to create bespoke protocols in the Fontan circuit. Quant Imaging Med Surg 7 (1):79–87. https://doi.org/10.21037/qims.2017.02.04
11. Nakagawa M, Ozawa Y, Nomura N, Inukai S, Shiba A, Sakurai K, Shimohira M, Shibamoto Y (2018) Investigation of an appropriate contrast-enhanced CT protocol for young patients following the Fontan operation. Jpn J Radiol 36 (3):215–222. https://doi.org/10.1007/s11604-018-0718-3
12. Duerden L, Abdullah H, Lyen S, Manghat N, Hamilton M (2020) Contrast circulation in adult fontan patients using MR time resolved angiography: application for CT pulmonary angiography. J Cardiovasc Comput Tomogr 14 (4):330–334. https://doi.org/10.1016/j.jcct.2019.12.035
13. Han BK, Rigsby CK, Leipsic J, Bardo D, Abbara S, Ghoshhajra B, Lesser JR, Raman SV, Crean AM, Nicol ED, Siegel MJ, Hlavacek A, Society of Cardiovascular Computed Tomography; Society of Pediatric Radiology; North American Society of Cardiac Imaging (2015) Computed tomography imaging in patients with congenital heart disease, Part 2: technical recommendations. An expert consensus document of the Society of Cardiovascular Computed Tomography (SCCT): endorsed by the Society of Pediatric Radiology (SPR) and the North American Society of Cardiac Imaging (NASCI). J Cardiovasc Comput Tomogr 9 (6):493–513. https://doi.org/10.1016/j.jcct.2015.07.007
14. Hong SH, Goo HW, Maeda E, Choo KS, Tsai IC; Asian Society of Cardiovascular Imaging Congenital Heart Disease Study Group (2019) User-friendly vendor-specific guideline for pediatric cardiothoracic computed tomography provided by the Asian Society of Cardiovascular Imaging Congenital Heart Disease Study Group: Part 1. imaging techniques. Korean J Radiol 20 (2):190–204. https://doi.org/10.3348/kjr.2018.0571
15. Goo HW (2010) State-of-the-art CT imaging techniques for congenital heart disease. Korean J Radiol 11 (1):4–18. https://doi.org/10.3348/kjr.2010.11.1.4
16. Goo HW (2012) CT radiation dose optimization and estimation: an update for radiologists. Korean J Radiol 13 (1):1–11. https://doi.org/10.3348/kjr.2012.13.1.1
17. Goo HW (2011) Individualized volume CT dose index determined by cross-sectional area and mean density of the body to achieve uniform image noise of contrast-enhanced pediatric chest CT obtained at variable kV levels and with combined tube current modulation. Pediatr Radiol 41 (7): 839–847. https://doi.org/10.1007/s00247-011-2121-4
18. Goo HW, Suh DS (2006) Tube current reduction in pediatric non-ECG-gated heart CT by combined tube current modulation. Pediatr Radiol 36 (4):344–351. https://doi.org/10.1007/s00247-005-0105-y
19. Goo HW (2018) Is it better to enter a volume CT dose index value before or after scan range adjustment for radiation dose optimization of pediatric cardiothoracic CT with tube current modulation? Korean J Radiol 19 (4):692–703. https://doi.org/10.3348/kjr.2018.19.4.692
20. Goo HW (2018) Comparison of chest pain protocols for electrocardiography-gated dual-source cardiothoracic CT in children and adults: the effect of tube current saturation on radiation dose reduction. Korean J Radiol 19 (1):23–31. https://doi.org/10.3348/kjr.2018.19.1.23

21. Han BK, Grant KLR, Garbrich R, Sedlmair M, Lindberg J, Lesser JR (2012) Assessment of an iterative reconstruction algorithm (SAFIRE) on image quality in pediatric cardiac CT datasets. J Cardiovasc Comput Tomogr 6 (3):200–204. https://doi.org/10.1016/j.jcct.2012.04.008
22. Nie P, Li H, Duan Y, Wang X, Ji X, Cheng Z, Wang A, Chen J (2014) Impact of sinogram affirmed iterative reconstruction (SAFIRE) algorithm on image quality with 70 kVp-tube-voltage dual-source CT angiography in children with congenital heart disease. PloS One 9 (3):e91123. https://doi.org/10.1371/journal.pone.0091123
23. Lee KB, Goo HW (2018) Quantitative image quality and histogram-based evaluations of an iterative reconstruction algorithm at low-to-ultralow radiation dose levels: a phantom study in chest CT. Korean J Radiol 19 (1):119–129. https://doi.org/10.3348/kjr.2018.19.1.119
24. Lee KB, Goo HW (2020) Comparison of quantitative image quality of cardiac computed tomography between raw-data-based and model-based iterative reconstruction algorithms with an emphasis on image sharpness. Pediatr Radiol 50 (11):1570–1578. https://doi.org/10.1007/s00247-020-04741-x
25. Goo HW (2017) Myocardial delayed-enhancement CT: initial experience in children and young adults. Pediatr Radiol 47 (11):1452–1462. https://doi.org/10.1007/s00247-017-3889-7
26. Leithner D, Wichmann JL, Vogl TJ, Trommer J, Martin SS, Scholtz JE, Bodelle B, De Cecco CN, Duguay T, Nance JW Jr, Schoepf UJ, Albrecht MH (2017) Virtual monoenergetic imaging and iodine perfusion maps improve diagnostic accuracy of dual-energy computed tomography pulmonary angiography with suboptimal contrast attenuation. Invest Radiol 52 (11):659–665. https://doi.org/10.1097/RLI.0000000000000387
27. Goo HW, Goo JM (2017) Dual energy CT: new horizon in medical imaging. Korean J Radiol 18 (4):555–569. https://doi.org/10.3348/kjr.2017.18.4.555

Tables

Table 1 Demographics and clinical characteristics of the patient population

		Group 1 (*n* = 38)	Group 2 (*n* = 41)	Group 3 (*n* = 36)
CT exam years		2006–2014	2014–2020	2012–2020
Age (years)		10.9 ± 6.3 (range, 3–25)	9.9 ± 7.2 (range, 3–24)	11.5 ± 7.9 (range 3–25)
Sex (male : female)		27 : 11	19 : 22	20 : 16
Cardiac defects	Complex functional single ventricle	23	26	29
	Tricuspid atresia	5	6	2
	Unbalanced atrioventricular septal defect	3	4	2
	Hypoplastic left heart syndrome	0	3	2
	Pulmonary atresia with intact ventricular septum	4	1	1
	Transposition of the great arteries with ventricular septal defect	3	1	0
Types of Fontan operation	Extracardiac conduit	32 (84.2%)	40 (97.6%)	34 (94.4%)
	Atriopulmonary connection	4 (10.5%)	0 (0.0%)	1 (2.8%)
	Lateral tunnel	2 (5.3%)	1 (2.4%)	1 (2.8%)
Metallic implant on CT scout	Pacemaker	7 (18.4%)	8 (19.5%)	6 (16.7%)
	Other metal	7 (18.4%)	9 (22.0%)	8 (22.2%)

Table 2 Cardiothoracic CT scan parameters

		Group 1 (*n* = 38)	Group 2 (*n* = 41)	Group 3 (*n* = 36)
CT scan type	Non-ECG-synchronized spiral scan	16 (single-source, 8; high-pitch dual-source, 8)	0	2 (single-source, 1; high-pitch dual-source, 1)
	Retrospectively ECG-gated spiral scan	13	19	18
	Prospectively ECG-triggered sequential scan	0	18	15
	Prospectively ECG-triggered high-pitch dual-source spiral scan	9	4	1
Tube voltage	70 kV	0	8	4
	80 kV	12	27	30
	100 kV	24	6	2
	120 kV	2	0	0
Radiation dose metric	Volume CT dose index (mGy)	6.3 ± 6.2	4.8 ± 4.7	4.1 ± 2.9
	Dose-length product (mGy·cm)	156.9 ± 173.4	108.4 ± 125.8	92.5 ± 84.8
	Effective dose (mSv)	2.6 ± 2.3	2.0 ± 1.8	1.5 ± 0.9

ECG electrocardiography

Table 3 Quantitative evaluation of the image quality and semi-quantitative evaluation of heterogeneous enhancement

		Group 1 (n = 38)	Group 2 (n = 41)	Group 3 (n = 36)	Group 1 vs. Group 2	Group 2 vs. Group 3	Group 1 vs. Group 3
Right internal jugular vein	Density (HU)	347.1 ± 179.0	361.8 ± 124.3	253.3 ± 56.6	p > 0.886	**p < 0.001**	**p < 0.004**
	SD (HU)	55.7 ± 35.1	40.6 ± 19.5	22.5 ± 9.6	**p < 0.018**	**p < 0.001**	**p < 0.001**
	Homogeneity	78.4% (29/37)	97.4% (37/38)	100.0% (32/32)	**p < 0.014**	p = 1.000	**p < 0.006**
	Sufficient enhancement	78.4% (29/37)	91.9% (34/37)	84.4% (27/32)	p > 0.102	p > 0.457	p > 0.525
Left internal jugular vein	Density (HU)	340.7 ± 176.7	366.6 ± 115.2	251.2 ± 60.8	p > 0.448	**p < 0.001**	**p < 0.005**
	SD (HU)	46.8 ± 27.1	43.6 ± 21.8	23.0 ± 7.8	p > 0.568	**p < 0.001**	**p < 0.001**
	Homogeneity	76.3% (29/38)	92.3% (36/39)	100.0% (33/33)	p > 0.053	p > 0.244	**p < 0.003**
	Sufficient enhancement	73.7% (28/38)	92.3% (36/39)	75.8% (25/33)	**p < 0.030**	p > 0.051	p > 0.841
Right SVC	Density (HU)	436.2 ± 149.5	308.5 ± 107.9	228.4 ± 47.1	**p < 0.001**	**p < 0.001**	**p < 0.001**
	SD (HU)	178.1 ± 112.9	60.2 ± 50.9	19.8 ± 8.6	**p < 0.001**	**p < 0.001**	**p < 0.001**
	Homogeneity	14.3% (5/35)	74.2% (23/31)	100.0% (29/29)	**p < 0.001**	**p < 0.005**	**p < 0.001**
	Sufficient enhancement	94.3% (33/35)	74.2% (23/31)	75.9% (22/29)	**p < 0.037**	p > 0.881	p > 0.066
Left SVC	Density (HU)	525.2 ± 228.9	254.8 ± 131.3	227.5 ± 39.8	**p < 0.005**	p > 0.470	**p < 0.043**
	SD (HU)	187.2 ± 92.4	48.5 ± 25.9	21.2 ± 6.8	**p < 0.027**	**p < 0.002**	**p < 0.016**
	Homogeneity	0.0% (0/5)	64.3% (9/14)	100.0% (12/12)	**p < 0.033**	**p < 0.043**	**p < 0.001**
	Sufficient enhancement	100.0% (5/5)	64.3% (9/14)	75.0% (9/12)	p > 0.256	p > 0.682	p > 0.514
IVC	Density (HU)	477.3 ± 204.2	676.7 ± 154.2	234.6 ± 85.1	**p < 0.001**	**p < 0.001**	**p < 0.001**
	SD (HU)	265.1 ± 109.8	307.1 ± 84.6	47.9 ± 62.9	p > 0.061	**p < 0.001**	**p < 0.001**

	Homogeneity	0.0% (0/38)	2.4% (1/41)	80.6% (29/36)	p = 1.000	**p < 0.001**	**p < 0.001**
	Sufficient enhancement	92.1% (35/38)	100.0% (41/41)	66.7% (24/36)	p > 0.106	**p < 0.001**	**p < 0.007**
Inferior cavopulmonary connection	Density (HU)	406.6 ± 190.2	579.3 ± 178.7	237.9 ± 46.6	**p < 0.001**	**p < 0.001**	**p < 0.001**
	SD (HU)	145.2 ± 106.4	215.5 ± 106.1	25.7 ± 23.7	**p < 0.004**	**p < 0.001**	**p < 0.001**
	Homogeneity	26.3% (10/38)	14.6% (6/41)	91.7% (33/36)	p > 0.196	**p < 0.001**	**p < 0.001**
	Sufficient enhancement	89.5% (34/38)	97.6% (40/41)	80.6% (29/36)	p > 0.189	**p < 0.023**	p > 0.281
Right pulmonary artery	Density (HU)	446.0 ± 192.3	430.1 ± 128.1	223.2 ± 42.8	p > 0.667	**p < 0.001**	**p < 0.001**
	SD (HU)	64.5 ± 48.2	101.2 ± 69.1	19.0 ± 6.4	**p < 0.008**	**p < 0.001**	**p < 0.001**
	Homogeneity	63.2% (24/38)	43.9% (18/41)	100.0% (36/36)	p > 0.086	**p < 0.001**	**p < 0.001**
	Sufficient enhancement	94.7% (36/38)	95.1% (39/41)	75.0% (27/36)	p = 1.000	**p < 0.012**	**p < 0.017**
left pulmonary artery	Density (HU)	420.0 ± 183.4	445.5 ± 203.4	220.5 ± 41.2	p > 0.560	**p < 0.001**	**p < 0.001**
	SD (HU)	59.1 ± 53.2	80.0 ± 66.9	20.2 ± 11.6	p > 0.128	**p < 0.001**	**p < 0.001**
	Homogeneity	71.1% (27/38)	73.2% (30/41)	100.0% (36/36)	p > 0.833	**p < 0.001**	**p < 0.001**
	Sufficient enhancement	89.5% (34/38)	87.8% (36/41)	69.4% (25/36)	p = 1.000	**p < 0.048**	**p < 0.032**
Ascending aorta	Density (HU)	440.6 ± 139.4	426.5 ± 113.2	237.7 ± 45.7	p > 0.623	**p < 0.001**	**p < 0.001**
	SD (HU)	12.6 ± 3.9	14.5 ± 4.7	13.3 ± 3.6	p > 0.063	p > 0.218	p > 0.473
	Homogeneity	100.0% (38/38)	100% (41/41)	100.0% (36/36)	N/A	N/A	N/A
	Sufficient enhancement	100.0% (38/38)	100% (41/41)	77.8% (28/36)	N/A	**p < 0.001**	**p < 0.002**
Ventricle	Density (HU)	417.2 ± 132.4	409.4 ± 110.7	229.3 ± 42.1	p > 0.775	**p < 0.001**	**p < 0.001**
	SD (HU)	12.6 ± 3.8	16.9 ± 6.7	15.0 ± 4.7	**p < 0.001**	p > 0.149	**p < 0.017**

	Homogeneity	100.0% (38/38)	100% (41/41)	100.0% (36/36)	N/A	N/A	N/A
	Sufficient enhancement	97.4% (37/38)	97.6% (40/41)	77.8% (28/36)	p = 1.000	**p < 0.011**	**p < 0.013**
Atrium	Density (HU)	420.4 ± 129.3	401.3 ± 110.0	228.7 ± 40.9	p > 0.478	**p < 0.001**	**p < 0.001**
	SD (HU)	16.2 ± 5.6	26.6 ± 17.4	16.7 ± 5.8	**p < 0.001**	**p < 0.001**	p > 0.691
	Homogeneity	100.0% (38/38)	87.8% (36/41)	100.0% (36/36)	p > 0.055	p > 0.057	N/A
	Sufficient enhancement	97.4% (37/38)	97.6% (40/41)	77.8% (28/36)	p = 1.000	**p < 0.011**	**p < 0.013**
Myocardium	Density (HU)	142.9 ± 53.7	151.8 ± 40.6	142.1 ± 26.7	p > 0.403	p > 0.212	p > 0.934
	SD (HU)	17.4 ± 9.6	21.9 ± 21.3	16.4 ± 7.6	p > 0.227	p > 0.128	p > 0.612
Image noise$_{air}$	SD (HU)	5.3 ± 1.5	6.4 ± 2.5	7.1 ± 1.6	**p < 0.017**	p > 0.141	**p < 0.001**
	Optimal noise	100.0% (38/38)	92.7% (38/41)	94.4% (34/36)	p > 0.241	p = 1.000	p > 0.233
SNR		86.2 ± 38.9	74.8 ± 39.0	34.3 ± 12.8	p > 0.196	**p < 0.001**	**p < 0.001**
Sufficient SNR		94.7% (36/38)	90.2% (37/41)	38.9% (14/36)	p > 0.676	**p < 0.001**	**p < 0.001**
CNR		56.1 ± 23.9	47.1 ± 26.2	12.9 ± 5.0	p > 0.114	**p < 0.001**	**p < 0.001**
Sufficient CNR		94.7% (36/38)	92.7% (38/41)	5.6% (2/36)	p = 1.000	**p < 0.001**	**p < 0.001**

CNR contrast-to-noise ratio, *HU* Hounsfield unit, *IVC* inferior vena cava, *N/A* not applicable, *SD* standard deviation, *SNR* signal-to-noise ratio, *SVC* superior vena cava

Figures

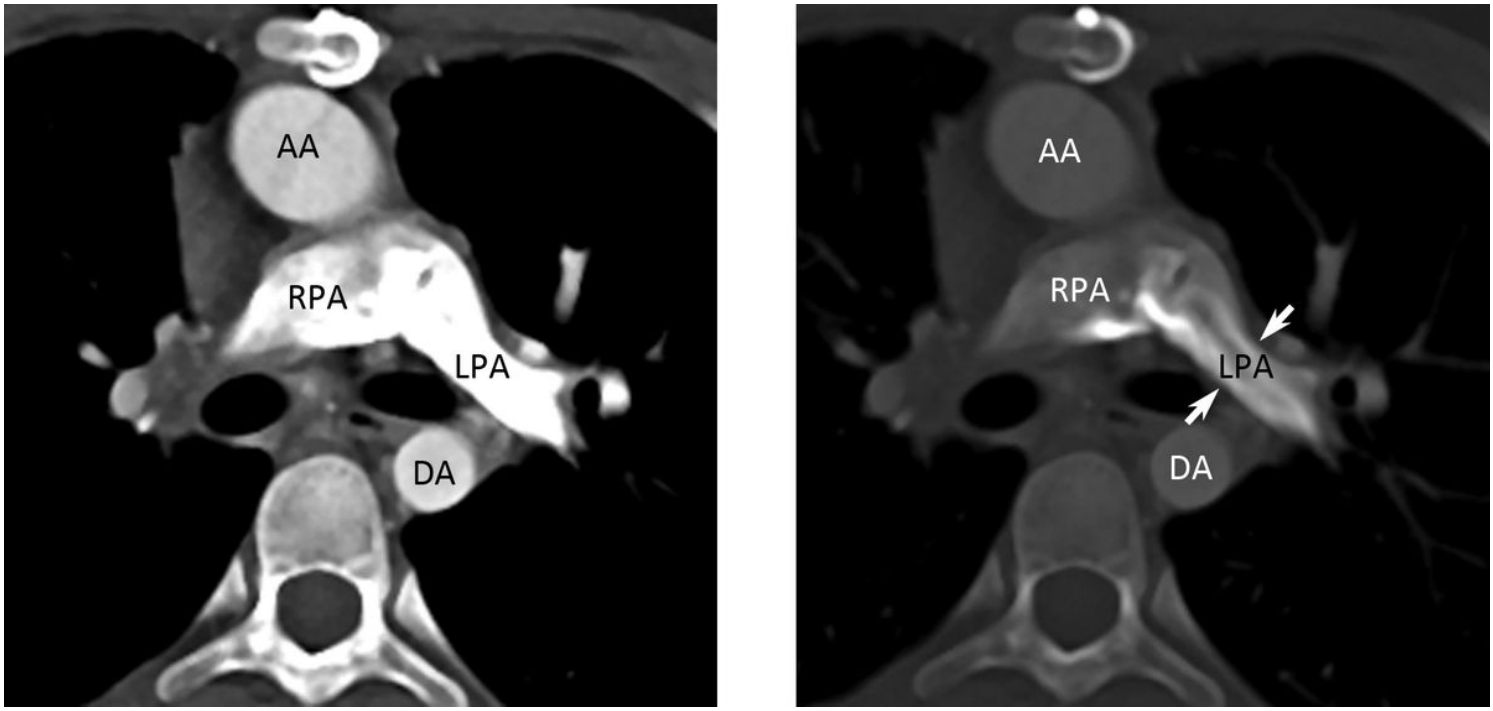

Figure 1

A 10-year-old girl with tricuspid atresia, transposition of the great arteries, and VSD who underwent the extracardiac conduit Fontan operation. a, b End-systolic axial CT images with mediastinal (a) and bone (b) window settings demonstrate that the visual evaluation of homogeneous enhancement in the Fontan pathway is inevitably erroneous and substantially influenced by the window settings of the CT images. Contrast enhancement in the LPA appears to be homogeneous in the mediastinal window setting (a), whereas it is heterogeneous (arrows in B) in the bone window setting (b). AA ascending aorta, DA descending aorta, LPA left pulmonary artery, RPA right pulmonary artery, VSD ventricular septal defect

Figure 2

A 25-year-old man with double outlet right ventricle, complete atrioventricular septal defect, and pulmonary stenosis who underwent the extracardiac conduit Fontan operation. a End-systolic axial CT image shows homogeneous enhancement in the SVC (asterisk) as well as the AA and DA. b Histogram obtained in the entire area (dotted red line in a) of the SVC demonstrates a single peak with a narrow base, which is in line with visually homogeneous enhancement. The standard deviation of the CT densitometry was approximately 16.2 HU. AA ascending aorta, DA descending aorta, HU Hounsfield units, SVC superior vena cava

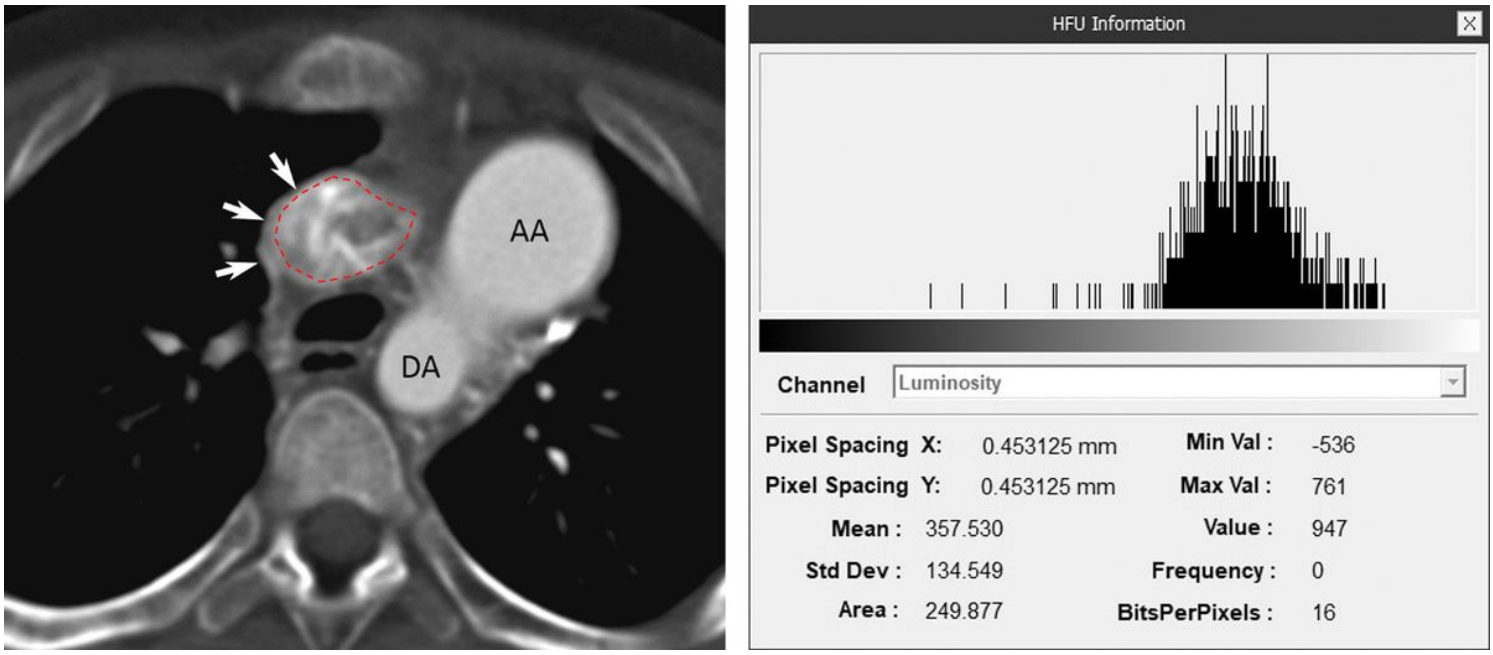

Figure 3

A 7-year-old boy with congenitally-corrected transposition of the great arteries, VSD, pulmonary atresia, and a hypoplastic right ventricle who underwent the extracardiac conduit Fontan operation. a End-systolic axial CT image reveals heterogeneous enhancement in the SVC (arrows), while homogeneous enhancement was noted in the AA and DA. b Histogram obtained in the entire area (dotted red line in a) of the SVC demonstrates a broad-based large peak, which is in line with visually heterogeneous enhancement. The standard deviation of the CT densitometry was approximately 134.5 HU. AA ascending aorta, DA descending aorta, HU Hounsfield units, SVC superior vena cava, VSD ventricular septal defect

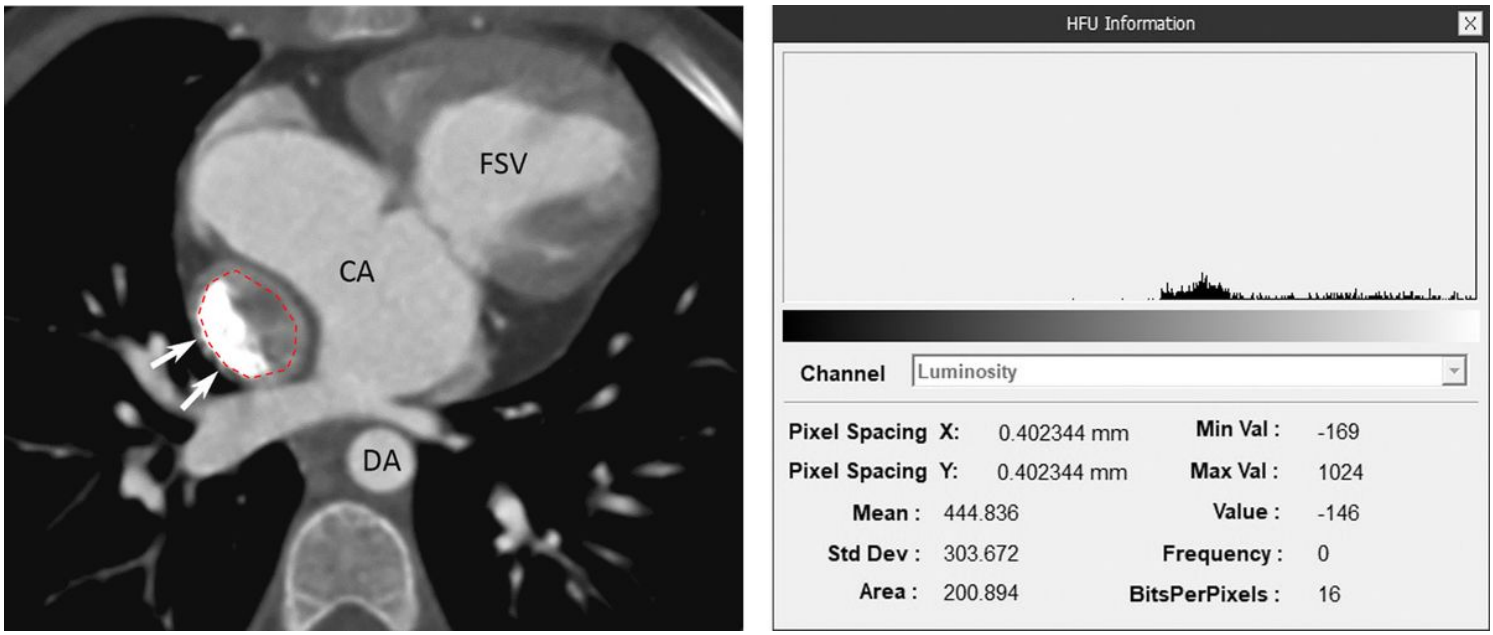

Figure 4

A 5-year-old girl with right isomerism, double outlet right ventricle, complete atrioventricular septal defect, pulmonary stenosis, and total anomalous pulmonary venous drainage who underwent the extracardiac conduit Fontan operation. a End-systolic axial CT image shows two unmixed areas of undiluted contrast agent and unopacified blood in the extracardiac Fontan conduit (arrows), while other cardiac chambers including the FSV and CA as well as the DA display homogeneous enhancement. b Histogram obtained in the entire area (dotted red line in a) of the extracardiac Fontan conduit demonstrates a broad-based small peak, which is in line with visually heterogeneous enhancement. The standard deviation of the CT densitometry was approximately 303.7 HU. CA common atrium, DA descending aorta, FSV functional single ventricle, HU Hounsfield units

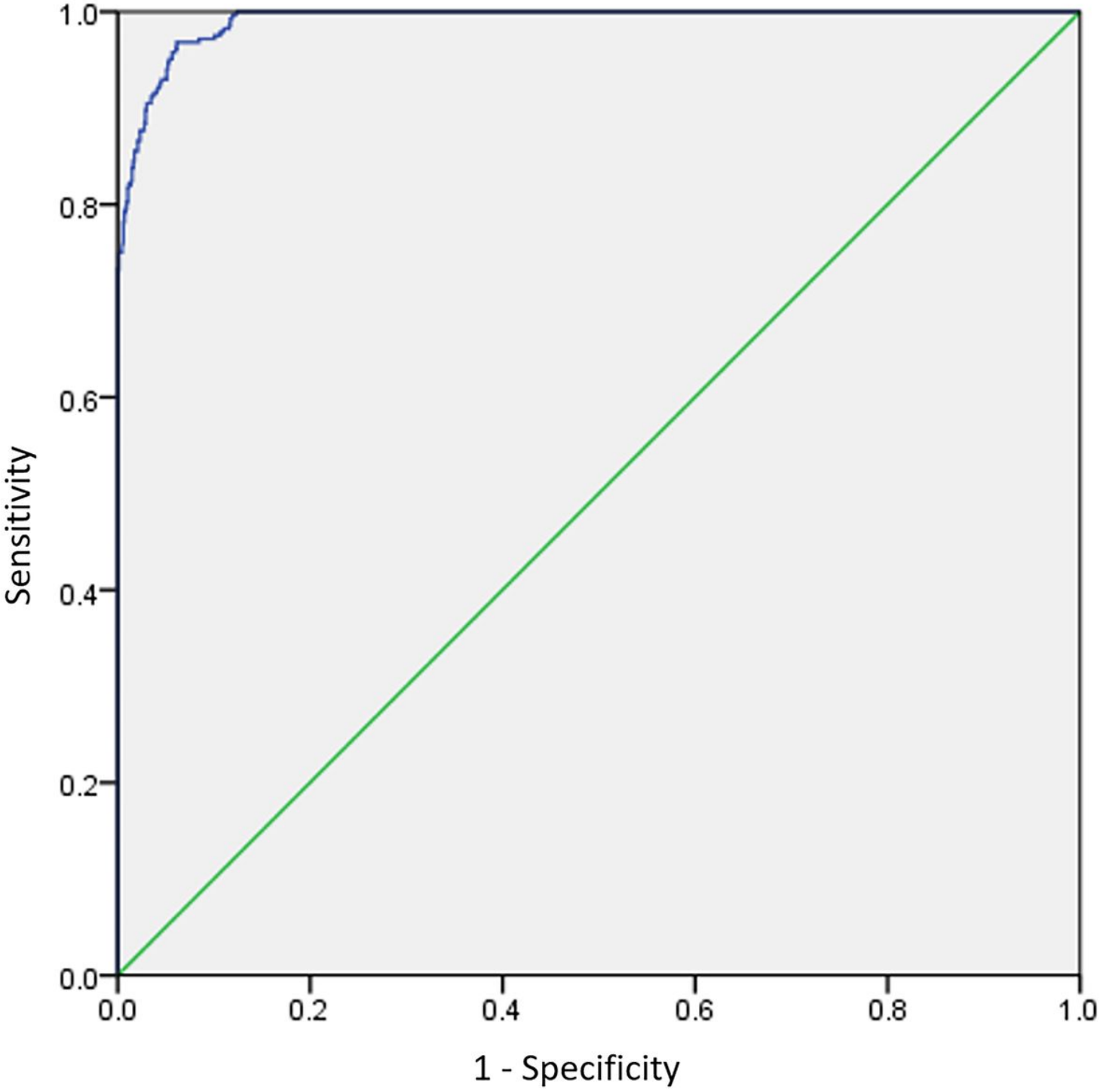

Figure 5

Receiver operating characteristic curve demonstrating the excellent diagnostic test of the standard deviation of the CT densitometry measured in the Fontan pathway in determining homogeneity of contrast enhancement (area under the curve = 0.991; 95% confidence interval, 0.988–0.994; $p < 0.001$).